



1 **A major waterfall landscape maintained by fog drip water**

2 **Lucheng Zhan^{1,2}, Jiansheng Chen^{3,4}, Chenming Zhang⁵, Tao Wang³, Ling Li⁵ and Pei Xin^{1,2}**

3 ¹ State Key Laboratory of Hydrology-Water Resources and Hydraulic Engineering, Hohai University,
4 Nanjing, 210098, China

5 ² College of Water Conservancy and Hydropower Engineering, Hohai University, Nanjing, 210098, China

6 ³ Geotechnical Research Institute, College of Civil and Transportation Engineering, Hohai University,
7 Nanjing, 210098, China

8 ⁴ College of Earth Sciences and Engineering, Hohai University, Nanjing, 210098, China

9 ⁵ School of Civil Engineering, the University of Queensland, St. Lucia, QLD 4072, Australia

10 *Correspondence to:* Jiansheng Chen (jschen@hhu.edu.cn) and Lucheng Zhan (luchengzhan@hotmail.com)

11



12 **Abstract**

13 The Chishui forest region in the southwest of China has a unique landscape with thousands of
14 waterfalls that produce a significant water yield even during and after a long dry period. However,
15 the sources of water for sustaining the waterfall landscape are poorly understood. We use stable
16 isotopes ^2H and ^{18}O to trace water in surface runoff and determine the runoff generation
17 mechanism in the catchments. Located on the pathway of water vapor from the neighboring
18 Sichuan Basin, the area is covered by a thick forest canopy above sandstone strata. The local
19 conditions combine to create a microclimate that favors formation of fogs at relatively high
20 frequencies. It was found that frequent fogs in this region act as a key water supplier for waterfalls
21 and play an important role in the regional hydrology. During the dry period starting from October,
22 waterfalls are mainly sustained by baseflow, 8-31% of which comes from frequent fog water
23 recharge. The waterfall landscape in the Chishui forest represents a unique characteristic of the
24 regional hydrological system in close connection with its geographical location, geology,
25 climatology and ecology.

26 **1 Introduction**

27 Many forest catchments experience a prolonged dry season with little or no rainfall, resulting in
28 significant surface water flow reduction and even dry riverbed in some cases (Jackson et al., 1995;
29 Liu et al., 2014; Querejeta et al., 2007). To adapt to the dry condition, local plants develop deep
30 roots, leaf withering and earlier flowering functions (Corbin et al., 2005; Goldstein et al., 2008).
31 In the southwest of China (Figure 1), there is a unique subtropical primeval forest called the
32 Chishui forest, where the vegetation coverage exceeds 90% with a wide range of species including
33 *Alsophila spinulosa* – a woody pteridophyte species surviving since the dinosaur age (Yang et al.,
34 2011). The forest is mainly underlain by Cretaceous or Jurassic quartz sandstone, which is different
35 from the surrounding areas (Qi et al., 2005). A large number of streams flow through the forest
36 region, resulting in the highest average drainage density (0.77 km/km^2) in China (Yang et al.,
37 2011). Located in the transition zone between the Yunnan-Guizhou Plateau and the Sichuan Basin,
38 this region is also characterized by a large number of faults and escarpments caused by past
39 geologic activities, which has led to the formation of thousands of waterfalls (Chen, 2003; Qi et
40 al., 2005). These waterfalls produce considerable water yield during the dry season when rainfall



41 is low (Chen, 2003). Another feature of the Chishui forest area is the frequent fog during all
42 seasons and thus the lowest solar radiation level in China (Xu et al., 2002).

43 Fog water droplets in the air can be intercepted by plant leaves. These droplets then coalesce
44 to form larger drops on the surface of the vegetation and fall to the ground. This process of water
45 input is called fog interception or cloud water interception (Bruijnzeel et al., 2011; Prada et al.,
46 2012). Previous studies showed that fog interception may affect significantly the hydrological
47 cycle and ecology in tropical montane and coastal cloud forests around the world (Bruijnzeel, 2002;
48 Bruijnzeel et al., 2011; Liu et al., 2014; Prada et al., 2016; Schmid et al., 2011). With more even
49 distribution throughout the year than rainfall, fog precipitation has long been assumed as an
50 essential additional water source in the relic laurel ecosystems of the Canary Islands (Aboal et al.,
51 2000; Garc ía-Santos and Bruijnzeel, 2011; Ritter et al., 2008) and in the coastal forests of
52 California (Dawson, 1998; Fischer et al., 2016; Ingraham and Matthews, 1990). The contribution
53 of the fog water to local water budget and plant use cannot be overlooked in the ecosystems of
54 tropical and temperate montane cloud forests as well as coastal ecosystems in major Mediterranean
55 climate zones (Fischer et al., 2016). Once the fog water falls to the ground, it becomes an important
56 water source for the forest ecosystem, contributing to soil water, aquifers and streams (Figueira et
57 al., 2013; Hutley et al., 1997; Ingraham and Matthews, 1988; Prada et al., 2012, 2016). Since a
58 conventional rain gauge is typically installed in the open field, it would not collect or record any
59 amount of fog drip water that occurs under the forest canopy (Nagel, 1956; Vogelmann et al.,
60 1968). The fog water's contribution is usually quantified indirectly, using methods such as
61 artificial fog collection (Klemm et al., 2012; Ritter et al., 2008), throughfall measurement (Holder,
62 2004; Uehara and Kume, 2012) and modelling techniques (Imteaz et al., 2011; Ritter et al., 2008).
63 The indirect methods rely on accurate rainfall and net precipitation measurements, which is
64 difficult to achieve, making it a challenge to separate contributions by fog and rain (Schmid et al.,
65 2011). Another problem is that the fog water contribution to the whole forest cannot be fully
66 characterized by the water volume measurement at individual sites (Ritter et al., 2008). For
67 example, Cavalier et al. (1996) measured fog water interception and rainfall at 14 stations in the
68 montane forests across the Central Cordillera of western Panama, and found that fog drip water
69 contributed between 2.4 and 60.6% of the total water input, subjected to a large degree of
70 uncertainty due to changes of altitude and exposure to the prevailing winds. To better estimate the
71 fog water contribution to local water budget, a better understanding of fog water-related



72 hydrological processes and a process-based quantification of fog water in groundwater and/or
73 surface water systems within the whole forest catchment is needed.

74 The fog water and rainwater exist in the hydrological system typically in a mixed form, which
75 makes it difficult to distinguish the two and trace them separately using traditional methods. As
76 the “fingerprint” of natural water, ^2H and ^{18}O stable isotopes have been widely applied to identify
77 different water sources in the hydrological cycle (Chen et al., 2014; Palacio et al., 2014; Zhan et
78 al., 2016). Due to different condensation conditions and processes, fog water and rainwater are
79 usually characterized by different isotopic compositions (Dawson, 1998; Gonfiantini and
80 Longinelli, 1962; Prada et al., 2016; Scholl et al., 2011). This offers an opportunity to distinguish
81 the fog water component in ecohydrological processes, and to quantify the ecological importance
82 of fog water to vegetation and its contribution to water budget in the cloud forests (Liu et al., 2014;
83 Schmid et al., 2011; Scholl et al., 2011; Zhan et al., 2017). Ingraham and Matthews (1988) used
84 isotopic methods to trace fog in northern Kenya and suggested that stable isotopes provided the
85 best tool available for tracing fog water movement into the groundwater system. Comparisons
86 between the results of a mass balance model based on stable isotopes and direct fog deposition
87 measurements indicated that the former method provides a good estimation of fog interception
88 under a wide range of conditions (Schmid et al., 2011).

89 However, it remains a question whether fog can provide water for thousands of waterfalls in
90 a subtropical inland area such as the Chishui forest. The forest region is underlain by red sandstone,
91 which is different from the surrounding areas. As a subtropical cloud forest, the Chishui forest may
92 also be affected significantly by the fog water input just like many coastal cloud forests around the
93 world (Bruijnzeel et al., 2011). However, the link of fog water to the forest’s unique waterfall
94 landscape and underlying hydrological processes are not well understood and require further
95 investigation. The annual rainfall in the area is not significantly different from the surrounding
96 areas (Figure S4 in supporting information). It is unclear why frequent fog appears in this region
97 and where the water through the large number of waterfalls in the dry period originates. To answer
98 these questions, several field investigations and water sampling campaigns over different temporal
99 and spatial scales were conducted in the study area. Water samples for rainfall, fog interception,
100 springs and surface runoff within the study area were collected and analyzed for ^2H and ^{18}O isotope
101 compositions. Using the methods of isotope hydrology, the water input from fog interception in



102 the Chishui forest region was examined and the underlying hydrological processes were analyzed,
103 based on which an overall conservative estimation of fog water contribution was derived.

104 **2 Materials and Methods**

105 **2.1 Study site**

106 Located in the northeast of Guizhou Province, southwest China, the Chishui forest lies in the
107 transition zone between the Yunnan-Guizhou Plateau and the Sichuan Basin (Figure 1a). It is one
108 of the best preserved mid-subtropical plant communities of China and is home for China's biggest
109 communities of *Alsophila spinulosa* (Figure 2f), a relict woody pteridophyte species which has
110 survived over the time since the Mesozoic (Xu et al., 2002; Yang et al., 2011). Characterized by
111 the subtropical humid climate, this region has an average annual rainfall of 1047mm, 80% of which
112 falls between April and September. The average relative humidity is about 82% and the mean
113 annual temperature is 18.1 °C, with 340-350 frost-free days per year. Because of frequent fog
114 events, the average sunshine time in the area is only 948.5-1292.5 h per year, making the local
115 solar radiation level the lowest in China (Xu et al., 2002).

116 Most areas of the Guizhou province belong to the karst landform dominated by limestone,
117 while the Chishui forest region developed on the larger and younger “Danxia landform” (red
118 sandstone uplands) in China (Qi et al., 2005). During the Jurassic period, the transition zone
119 between the Yunnan-Guizhou Plateau and the Sichuan Basin was a big inland lake surrounded by
120 limestone. Through tens of millions of years of sedimentation, red sandstone gradually covered
121 the bed of the lake. About 30 million years ago, following the Indian plate's subducting against
122 the Eurasian plate, the Yunnan-Guizhou region was gradually uplifted into a plateau, together with
123 the uplift of the sandstone formation in the lake area. Under the combined influence of hydraulic
124 erosion, gravitational collapses and weather denudation, high steep red cliffs gradually developed
125 along both sides of the stream valleys, forming a unique landform in the area (Qi et al., 2005; Li
126 et al., 2013a). Most of the exposed strata are sedimentary rocks, which are composed of Jurassic
127 and Cretaceous strata (99%), and quaternary strata (1%). The Jurassic and Cretaceous strata are
128 characterized mainly by lacustrine sediments such as red quartz sandstone or siltstone (Li et al.,
129 2013b) (Figure 2c and g). Geological activity in the junction of the Yunnan-Guizhou Plateau and
130 the Sichuan Basin results in a large number of faults and escarpments (Qi et al., 2005). Further



131 geological information about the study area can be obtained from the China Geological
132 Information Data Centre (<http://geodata.ngac.cn/>).

133 The study site within the Chishui forest region is a 2,390 km² catchment area (Figure 1c) near
134 the downstream reaches of the Chishui River, which is a tributary of the Yangtze River (Figure
135 1b). The elevation in the entire catchment decreases from about 1790 m on the southeast corner to
136 220 m on the northwest corner. This area has a highly developed surface runoff system, and covers
137 mainly the Datong and Fengxi subcatchments (Figure 1c), with the highest drainage density
138 reaching 1.37 km/km². Most waterfalls in the Chishui forest region concentrate in these two sub-
139 catchments. The Shizhangdong waterfall (Figure 2e), located in the upper reach of the Fengxi
140 stream, is the largest waterfall in the area and the whole Yangtze River basin. It is 80 m in height
141 and 76.2 m in width, and has a drainage area of only 170 km² but a discharge reaching 320 m³/s
142 in the rainy season (Chen, 2003; Qi et al., 2005). The Datong catchment has the second largest
143 waterfall, the Sidonggou waterfall group, which has four levels with a maximum height of 50 m
144 and a maximum width of 40 m. The main waterfall area is densely forested, with vegetation
145 coverage greater than 95% (Figure 2d). Groundwater flows through clastic rock fissures in a
146 sandstone aquifer. Although the rainfall concentrates in the summer, the waterfalls still produce
147 considerable discharge during the dry period from October to March according to long-term field
148 observations by Chen (2003).

149 **2.2 Water sampling**

150 The first field investigation was carried out with surface water samples collected across the entire
151 Chishui River basin (Figure 1b) from June 5 to 12, 2011. Before this sampling work, the
152 southeastern region of China had experienced a serious drought that started in January 2011 and
153 lasted for nearly 5 months. Affected by this drought event, the rainfall amount from January to
154 May 2011 at a meteorological station near the Chishui forest was only 187 mm, which is the lowest
155 of the same period during 1981-2015 (Figure S1). Through the field investigation, we observed
156 obvious water shortage in stream flow within the upper reaches of the Chishui River because of
157 the drought (Figure 2a). There was no occurrence of fog in the upstream areas of high elevations.
158 In contrast, dense fog still occurred regularly in the Chishui forest region (downstream) in the early
159 morning, especially in the Datong and Fengxi catchments (Figure 2b). The ground was moist and
160 waterfalls flowed strongly, showing little impact by the drought (Figure 2b and c). Clean brown



161 5-ml vials with good airtightness were used for water sampling. Immediately after the water
162 sample was taken, the vial was capped and tightly sealed with tape to minimize possible
163 evaporation. In total, thirty-six water samples were collected during the first sampling campaign:
164 ten from the mainstream of the Chishui River and twenty-six from the tributaries (Figure 1b).
165 Twelve samples were taken in the forest area, including three waterfall samples. Geographical
166 coordinates and elevations of all sample locations were recorded at the site using the global
167 positioning system.

168 Another, more detailed field investigation with sampling focusing on the Chishui forest
169 catchment (Figure 1c) was conducted from December 22 to 26, 2014 during the dry season.
170 Sampling covered fog drips, springs, streams, waterfalls and rivers. Extensive sampling was
171 conducted in the catchments of Datong and Fengxi streams, especially in three key waterfall
172 landscape areas – Shizhangdong (Figure 1f), Sidonggou (Figure 1d) and Yanziyan (Figure 1e).
173 Water samples of the mainstream and tributaries of the Chishui River in the forest catchment
174 region were also taken. Every morning during the field trip, the forest was covered by fog (Figure
175 2d), which was gradually dispersed by sunshine later in the day. The sandstone wall under the
176 canopy of the forest was found to be very moist (Figure 2g) and it could be easily seen that fog
177 water kept dripping from the canopy to ground. Exposed rock surfaces were wetted everywhere
178 by spring water flowing from sandstone fissures (Figure 2h). Waterfalls with different scales and
179 shapes could be found on the cliffs of sandstone. Fog water samples were taken at different
180 elevations by collecting water drops on the tips of plant leaves under the forest canopy using clean
181 5-ml vials (Figure 2i). There was no rain during the five sampling days (Figure S1) so that the
182 water samples collected represented fog interception by the forest canopy. To prevent evaporation
183 caused by increasing air temperature, fog water sampling was taken in early morning (before 9:00
184 am). Samples of spring water flowing from the sandstone fissures and surface water including
185 streams, waterfalls and the Chishui River mainstream were also collected using 5-ml vials. In total,
186 eighty water samples were collected during the second sampling campaign.

187 Sampling was also conducted from June to December 2015 to collect water samples twice a
188 month from the Datong and Fengxi streams before they join the Chishui River (Figure 1c). The
189 stream water samples were collected using 380-ml polyethylene bottles sealed and kept
190 refrigerated at approximately 4 °C. A rainwater collector was installed at an open site of the study
191 area (Figure 1c, elevation: 265 m.a.s.l.) for collecting monthly rainfall water samples from January



192 2015 to December 2015. The collector was made of a 15-cm diameter polyethylene funnel draining
193 to a 10-L polyethylene bottle, containing a layer of oil film to minimize evaporation. At the end of
194 every month, the rainwater was sampled with a sealed 380-ml polyethylene bottle and then sent to
195 the laboratory for isotope analysis together with stream water samples. In total, 28 stream water
196 samples (14 for each stream) and 12 monthly rainwater samples were collected in 2015.

197 **2.3 Stable isotope analysis**

198 After each sampling campaign, water samples were immediately sent to Hohai University (Nanjing,
199 China) for the analysis of hydrogen and oxygen isotopes in the State Key Laboratory of
200 Hydrology-Water Resources and Hydraulic Engineering. The stable isotopic composition of
201 hydrogen was determined using an automated on-line elemental analyser (FlashEA HT) connected
202 to a Mat 253 mass spectrometer. This technique involved the reaction of sample water with carbon
203 at 1450 °C in a helium carrier gas. The product gases (H₂ and CO) were separated in a gas
204 chromatograph and analysed in the spectrometer for the hydrogen stable isotopic composition. For
205 the analysis of oxygen isotopic composition, water samples placed in vials were first flushed with
206 0.3% CO₂ for 10 minutes and then equilibrated with the 0.3% CO₂ headspace for 20 h at the
207 constant temperature of 25 °C. Following the equilibration, vials were then inserted into a
208 GasBench II system connected to the Mat 253 mass spectrometer. Hydrogen and oxygen isotopic
209 rates were reported in the standard δ -unit in parts per thousand with respect to the Vienna Standard
210 Mean Ocean Water. Analytical precisions were determined to be $\pm 2\text{‰}$ and $\pm 0.1\text{‰}$ for $\delta^2\text{H}$ and
211 $\delta^{18}\text{O}$, respectively.

212 The local meteoric water line (LMWL) in the study area was fitted using the monthly
213 precipitation isotope data. Data for daily rainfall in the sampling years, historical data (1981-2010)
214 for monthly average relative humidity, rainfall amount, daily temperature range, wind speed and
215 wind direction in the study area and surrounding regions were obtained from the China
216 Meteorological Database (<http://data.cma.cn/>). By comparing the isotopic compositions of
217 monthly precipitation from 2015 with the water samples collected during the three sampling
218 campaigns, key water sources and associated hydrological processes in the study area were
219 examined. Based on the analysis of rainfall-runoff process in the Datong and Fengxi catchments,
220 the two-compartment linear mixing model of Phillips and Gregg (2001) was used to estimate the
221 proportion (X) of fog water in the baseflow of the main waterfall catchments,



222

$$X = \frac{\delta_{baseflow} - \delta_{rain}}{\delta_{fog} - \delta_{rain}}$$

223 where $\delta_{baseflow}$, δ_{fog} and δ_{rain} are the isotopic values ($\delta^2\text{H}$ or $\delta^{18}\text{O}$) of baseflow, fog water and
224 rainwater, respectively.

225 3 Results and discussion

226 3.1 Isotopic anomaly of the Chishui forest catchment discovered during the basin-scale 227 investigation

228 Isotopic results (supporting information Database) of water samples collected across the entire
229 Chishui River basin in 2011 showed an enrichment of heavy isotopes in the mainstream of the
230 Chishui River from upstream to downstream (Figure 3b&c, section A-B-C-D as shown in Figure
231 3a). With decreasing elevation from 1455 m at No.1 to 226 m at No.12, the $\delta^2\text{H}$ and $\delta^{18}\text{O}$ values
232 of the mainstream increased from -55.6‰ and -8.63‰ to -41.1‰ and -6.32‰ , with elevation
233 gradients of $-1.18\text{‰}/100$ m and $-0.19\text{‰}/100$ m, respectively. In the upstream catchment (A-B)
234 before the river flowed into the Chishui forest area, the isotopic values of the mainstream increased
235 slowly with the discharge of tributaries. Due to the altitude effect on isotopes in precipitation,
236 surface water from the tributaries became more enriched in heavy isotopes (Figure 3 c&d) with
237 the catchment elevation decreasing towards the downstream (Figure 3a). However, when the river
238 flowed through the forest region (B-D), its isotopic composition changed dramatically, showing a
239 slow depletion followed by a sudden enrichment. The isotopic depletion in section B-C might be
240 caused by input of local rainwater of depleted heavy isotopes due to the quickly increasing
241 elevation in the southeastern part of the forest catchment (Figure 1c). Further downstream, the
242 surface water in the Datong and Fengxi stream catchments (main waterfall region) became much
243 more enriched in heavy isotopes than that in the upstream areas (Figure 3c), leading to the
244 subsequent, rapid isotopic enrichment of mainstream from section C to D (No.11 to 12). This
245 phenomenon seems not consistent with the altitude effect of precipitation isotope because the
246 average elevation in the Datong and Fengxi catchments is higher than that of section B-C, with the
247 highest elevation reaching up to 1790 m, approximating that of the headstream of the Chishui
248 River. In this section (C-D), the elevation gradients for $\delta^2\text{H}$ and $\delta^{18}\text{O}$ in the mainstream reached –
249 $29.0\text{‰}/100$ m and $-4.59\text{‰}/100$ m, respectively, much greater than those of the entire mainstream



250 in the Chishui River basin ($-1.18\text{‰}/100\text{ m}$ and $-0.19\text{‰}/100\text{ m}$). The large isotopic change after
251 the river flowed through the main waterfall region indicated that surface water in the Datong and
252 Fengxi catchments may have a water source of a different isotopic composition from that of local
253 rainwater.

254 Based on the isotopic results of rainfall samples collected in the study area in 2015, the local
255 meteoric water line (LMWL) in the Chishui forest was fitted as $\delta^2\text{H} = 8.65\delta^{18}\text{O} + 17.78$ ($n=12$,
256 $r^2=0.98$) (supporting information Figure S2). As shown in Figure 3b, isotope values of surface
257 water in the upstream Chishui River basin were scattered on or below the LMWL and formed
258 SWL1 ($\delta^2\text{H} = 5.44\delta^{18}\text{O} - 7.29$, $r^2=0.87$) with a smaller slope than LMWL, indicating that it was
259 sourced from rainfall and sometimes affected by evaporation. However, in the forest region,
260 especially around the main waterfalls, isotope data were largely scattered above the LMWL along
261 SWL2 ($\delta^2\text{H} = 4.58\delta^{18}\text{O} - 4.33$, $r^2=0.80$) significantly different from SWL1 (Figure 3b), indicating
262 that the Datong and Fengxi stream catchments had a water source that is different from the water
263 source in the upstream basin. Based on these basin scale isotope results and daily observations of
264 fog formation and dripping during the field trip, we hypothesized that fog water might affect the
265 isotopic composition of water in the waterfall areas. To verify this hypothesis, the second field
266 investigation was carried out in December 2014 with a focus on the isotope characteristics in the
267 Chishui forest catchment (Figure 1c).

268 **3.2 Evidences for fog water recharge during the investigation focusing on the forest** 269 **catchment**

270 With $\delta^2\text{H}$ and $\delta^{18}\text{O}$ values ranging from 3.5‰ to 31.5‰ and -3.62‰ to 0.93‰ (supporting
271 information Database), respectively, the fog water was much more enriched in heavy isotopes than
272 the December rainwater (Figure 4), similar to the finding of previous studies on the isotopic
273 composition of fog water (Corbin et al., 2005; Ingraham and Mark, 2000; Ingraham and Matthews,
274 1990; Scholl et al., 2011). However, the data points for all fog water samples appeared above the
275 LMWL, which is different from the results in coastal areas where fog forms from water vapor
276 coming directly from the ocean evaporation and hence has an isotope composition following the
277 meteoric water line (Corbin et al., 2005; Ingraham and Matthews, 1990). Deuterium excess,
278 defined as $d\text{-excess} = \delta^2\text{H} - 8\delta^{18}\text{O}$, can be used as an indicator of the origin of the water vapor
279 (Liu et al., 2008; Prada et al., 2015). The fog water in the Chishui forest was characterized by an



280 average d-excess of 29.0‰, much higher than the global mean value (10‰) and that of the local
281 rainwater in December (14.7‰). This indicates that the fog formed from condensed water vapor
282 produced by different regional recycled meteoric water from evaporation (Froehlich et al., 2008;
283 Liu et al., 2005, 2007). The fog water isotope line (FWL: $\delta^2\text{H} = 5.63\delta^{18}\text{O} + 26.24$, $r^2=0.78$; Figure
284 4) had a lower slope than that of LMWL, indicating that the fog water might have experienced
285 evaporation. The fog droplets in the air have smaller sizes and higher surface/volume ratios than
286 those of rain droplets, so they are more subjected to the evaporation effect despite relatively high
287 local air humidity (Prada et al., 2015).

288 Consistent with the results from 2011, water samples collected from the mainstream of the
289 Chishui River and the forest catchment in December 2014 showed significant differences in
290 isotopic compositions (Figure 4), indicating again a different water input component in the forest
291 area. The box plots showed similar variation ranges and average values of $\delta^{18}\text{O}$ and $\delta^2\text{H}$ among
292 samples collected from waterfalls, streams and springs, indicating the linkage of the surface water
293 (in waterfalls and streams) with spring water (groundwater). Water in the forest catchment showed
294 little isotopic evidence for evaporation, which is consistent with the high humidity in the forest
295 (supporting information Figure S3). Twelve of seventeen spring water samples, nineteen of
296 twenty-three stream samples and twelve of fifteen waterfall samples showed isotopic
297 characteristics above the LMWL. The d-excess values of waterfalls (15.0‰), streams (15.6‰)
298 and springs (15.0‰) were higher than the volume-weighted mean value (11.8‰) of local rainfall
299 and that of the Chishui river mainstream (11.9‰) (Figure 4d), indicating again an additional
300 recycled water component contributing to water balance in the forest area. Rainwater in the rainy
301 season (May to September) had d-excess values around 10‰ (supporting information Database),
302 which could not explain the recycled water component in the surface water and groundwater.
303 Rainwater in April was plotted above the LMWL and had a relatively high d-excess, but it was
304 long before the actually sampling date and could not explain the similar findings in both June 2011
305 and December 2014. Although the data points of local rainfall isotopes in some winter months
306 (November to January) also had higher d-excess values, the small rainfall amount (only 93 mm
307 from November 2014 to January 2015) in these months would not be sufficient to generate
308 significant runoff and affect the isotopic composition of surface water in streams and waterfalls. A
309 more likely explanation for the higher isotopic values and d-excess of surface and groundwater in



310 the Chishui forest catchment, other than the rain-sourced water (Figure b, c&d), is the input to
311 catchment from fog drip water in addition to local rainfall.

312 Through a review of 68 studies on a number of the world's mountain belts, Poage and
313 Chamberlain (2001) concluded that there is a consistent linear relationship between isotopic values
314 and corresponding elevations of water sourced from precipitation, with about 80% of the
315 coefficients of determination (r^2 values) in these studies greater than 0.7. In the present study, fog
316 water samples were collected at different elevations ranging from 250 m to 1140 m; but unlike
317 precipitation, there was no correlation between fog water isotopic composition and elevation
318 (Figure 5), indicating different isotope fractionation processes for rainwater and fog water
319 condensation. Spring, stream and waterfall water samples were also collected at a wide range of
320 elevations from 235 m to 1152 m (supporting information Database). However, the r^2 values for
321 the linear regression of water isotopes with elevations for these samples were only 0.32 and 0.28
322 for $\delta^2\text{H}$ and $\delta^{18}\text{O}$, respectively (Figure 5). Moreover, the fitted $\delta^{18}\text{O}$ lapse rate in the Chishui forest
323 region was only 0.1‰ /100 m, much lower than the rates for most regions of the world \sim 0.28‰
324 /100 m (Poage and Chamberlain, 2001). Since no elevation effect was found in the isotopic
325 composition of fog water, the weak isotope-elevation correlation and small isotopic lapse rate in
326 groundwater and surface water may be linked to the fog water input. The isotopic values the river
327 mainstream increased quickly over the elevation range from 250 to 220 m where the mainstream
328 received water from the Fengxi and Datong streams (Figure 5), indicating that fog water input
329 happened mainly in these two subcatchments.

330 The two isotopic investigations in 2011 and 2014 revealed that surface water and groundwater
331 (spring) in the forest region and upstream catchments were characterized by significantly different
332 stable isotope compositions. The unusual isotopic characteristics in the forest, especially the
333 waterfall-concentrated regions (Datong and Fengxi stream catchments), can be linked to the input
334 of fog drip water, which also explained why the waterfall landscape remained wet even during
335 drought conditions.

336 **3.3 Rainfall-runoff process in the waterfall-concentrated catchments**

337 The third sampling campaign was carried out to continuously monitor the isotopic compositions
338 in the Datong and Fengxi streams (Figure 1c), which were fed by waterfalls in the corresponding
339 catchments. According to the meteorological data (Figure 6), the annual precipitation at the study



340 site in 2015 was 1122 mm. The rain season in the region lasts from April to September, producing
341 nearly 80% of the total annual rainfall. The seasonal isotopic variation of the streams were much
342 smaller than that of the monthly rainfall (Figure 6). Although the Fengxi stream was more depleted
343 in heavy isotopes than the Datong stream in most months due to the higher altitudes in the Fengxi
344 catchment, both streams had a very similar temporal variation pattern in isotopic values. From
345 June to October, the isotopic compositions fluctuated significantly, but became relatively stable
346 from October to December. Streams usually consist of two hydrograph components: (1) surface
347 and near-surface quickflow in response to recent rainfall events, and (2) baseflow – water input
348 from persistent, slowly varying sources that maintains streamflow between rainfall events (Klaus
349 and McDonnell, 2013; Meyer, 2005; Muñoz-Villers and McDonnell, 2012). During the rainy
350 season, the rainfall rate was large enough to generate a considerable discharge of quickflow into
351 the Datong and Fengxi streams and cause obvious isotopic fluctuations of the stream water. When
352 the rainfall became small in the dry season, however, the streams in the catchment were maintained
353 by baseflow and displayed relatively stable isotopic compositions. The isotopic compositions of
354 the streams in December 2015 were similar to those in December 2014, indicating the stability of
355 isotopic compositions of baseflow. The isotopic compositions of the streams in June 2011 appeared
356 to be similar to those of base flow after a drought period in the area.

357 A phase lag of isotopic signal in the streamflow compared with the rainwater (input to the
358 catchment) can be found, indicating a transit time of rainwater in the catchment. From June to
359 early August, a depleting trend of isotopes ^2H and ^{18}O was observed in both the Datong stream and
360 Fengxi stream, corresponding to the overall isotopic depletion of rainfall from March to July with
361 a lag. Similarly, stream isotopic values between early August and middle September showed a
362 delayed trend similar to that of rainwater isotopes from July to September. It seems that the lag
363 time between rainfall and streamflow had a trend of decreasing from the beginning of the rainy
364 season to the period from September to October, when isotopes of stream water and rainwater
365 varied almost simultaneously. From October to December, although the isotopes in rainwater
366 changed significantly, there was little variation in isotopes of stream water, indicating little direct
367 contribution of rain to the streamflow in the dry season. The rainy season in the Chishui forest
368 begins in April after a five-month long dry period. Because of the little rainfall in the dry season,
369 water stored in the unsaturated zone and aquifers greatly decrease over this period. It can be
370 assumed that at the beginning of the rainy season, the rainwater infiltrates to recover the soil



371 wetness conditions before generating runoff (Muñoz-Villers and McDonnell, 2012). As a
372 consequence, the observed delay time from rainfall to surface water was longer in the early stage
373 of the rainy season in the Chishui region. As the groundwater level, as well as the rainfall intensity
374 increased from June to October, rainwater could reach the streamflow more quickly. After October,
375 rainfall greatly decreased and became again a minor contributor to the streams.

376 The Chishui forest catchment is underlain by sandy soils and substrate of high permeability,
377 making it easier for rainwater to infiltrate and recharge the groundwater. Streamflow in the
378 montane catchments is usually primarily composed of near-surface runoff and baseflow of a longer
379 residence time. Typically the baseflow comprises a long-term mixture of rainfall, and its isotopic
380 composition can be estimated by the volume-weighted mean value of rainfall isotopes over a long
381 period (Goni, 2006). If rainfall is the only water source for the catchment, the isotopic composition
382 of baseflow should be similar to the volume weighted mean (VWM) isotopic value of annual
383 rainfall ($\delta^2\text{H} = -51.6\text{‰}$, $\delta^{18}\text{O} = -7.94\text{‰}$) or that of the wet season rainfall ($\delta^2\text{H} = -57.4\text{‰}$, $\delta^{18}\text{O}$
384 $= -8.55\text{‰}$) and the isotopic composition of stream water should fluctuate around this isotopic
385 value. However, as shown in Figure 6, stream water was more enriched in heavy isotopes than
386 VWM values in most months. This suggests that the baseflow in the Chishui forest catchments
387 was not just a mixture of rainwater from different rainfall events, but a mixture of both rainwater
388 and a considerable amount of fog drip water.

389 **3.4 Estimated contribution of fog water to the main waterfall catchments and comparison** 390 **with results from other areas around the world**

391 As discussed above, it is hypothesized that the baseflow in the Datong and Fengxi catchments is
392 likely a mixture of rainwater and fog drip water. Based on this hypothesis, the proportion (X) of
393 fog water in baseflow for each catchment can be estimated by the two-compartment linear mixing
394 model (Phillips and Gregg, 2001), with isotopic compositions of rainwater and fog water as two
395 end members. Isotopic values of Datong and Fengxi stream water samples collected in mid-
396 December 2015 were used to approximate the isotopic composition of baseflow in the
397 corresponding catchments. The isotopic composition of rainwater input was represented by the
398 volume weighted mean (VWM) isotopic values of monthly rainfall collected in 2015. Since fog
399 water samples were not collected over the whole year, the exact long-term isotopic input of fog
400 water could not be determined. In the mixing model, the $\delta^2\text{H}$ and $\delta^{18}\text{O}$ values of baseflow and



401 rainwater input were held constants while the values of each fog water sample were used in the
402 calculation carried out for all fog water samples (10 in total for Datong and 8 for Fengxi). This
403 resulted in a number of estimates of the fog water contribution (X) to baseflow according to the
404 sample number for both catchments. The average, standard error and ranges of calculated fog water
405 proportions are summarised in Table 1.

406 Fog water's proportions in baseflow calculated by $\delta^2\text{H}$ are similar to those by $\delta^{18}\text{O}$ as
407 expected. Generally, the estimation shows that fog water accounts for a significant amount of the
408 baseflow in the Datong and Fengxi catchments, with the proportion of 16-31% and 8-16%,
409 respectively. Assuming that the proportion of fog water in the baseflow reflects the ratio of total
410 annual fog water to total annual rainfall, we can estimate the annual fog water input to the area to
411 be 98–504 mm in 2015 when the total annual rainfall was 1122 mm. The estimated fog water input
412 in the Fengxi catchment appeared to be smaller than that in the Datong catchment. This difference
413 may be caused by the simplification that two catchments have the same rainfall amount and rainfall
414 isotopic input. In reality, the Fengxi catchment should have a higher rainfall rate with more
415 depleted rainwater because of its higher altitude, and thus the proportion of fog water component
416 in its baseflow should be higher.

417 The above analysis and estimates of the fog water contribution are subjected to uncertainties
418 associated with a number of factors. First, the rainwater samples were collected in the study area
419 with elevation of only 265 m.a.s.l., much lower than the Datong and Fengxi catchments. Because
420 of the altitude effect on rainfall isotopes, the actual isotopic values of the rainfall end member (that
421 should be used in the mixing model) are likely to be smaller than the values used for the analysis
422 and estimation, which would lead to a higher fog water proportion. Secondly, the baseflow isotope
423 values used in the analysis were based on the stream water samples collected in mid-December
424 2015 and the rainwater values based on the volume-weighted mean of rainfall data also from 2015;
425 however the fog water data were collected from December 2014. Therefore, the real long-term
426 isotopic input from fog water was not determined. The water vapor that was condensed to fog
427 droplets mainly came from regional evapotranspiration, which originated from rainwater. The
428 isotopic composition of fog water would vary seasonally like the rainwater (Scholl et al., 2011).
429 In December 2014 when the fog water was collected, the rainwater was the most enriched in heavy
430 isotopes in the year (Figure 6), which would have resulted in high isotope values for the collected
431 fog water sample (higher than average). This would have led to underestimates of the overall fog



432 water contribution to the baseflow and the catchments. In short, while the estimates presented in
433 Table 1 are subjected to uncertainties, they are likely to represent the lower bound of the fog water
434 contribution to the Chishui forest region.

435 The estimated amount of fog water as part of the water balance in the study area is similar to
436 those found in other fog-affected forests around the world. Table 2 lists the results of 13 studies
437 (including the present one) quantifying fog water captured by forests using different approaches
438 such as artificial fog collecting, throughfall measurement and modelling techniques. Located
439 between 30° S - 41° N and 124° W - 152° E, most of these forests were found to have a general
440 fog deposition rate of a few hundred millimetres per year. The amount of water produced by fog
441 deposition depends partly on vegetation properties, climatic factors and terrain characteristics
442 (Ritter et al., 2008). Although most of these forests are located in coastal areas, two of them (Hutley
443 et al., 1997; Ritter et al., 2008) shown in Table 2 have the subtropical humid climate and are of the
444 broad-leaved forest type, similar to the Chishui forest, and with annual fog deposition amount (450
445 mm and 251-281 mm) close to the estimation in this study.

446 **3.5 Conceptual model of fog formation and recharge mechanism in the Chishui forest** 447 **catchment**

448 Composed of tiny condensed liquid water droplets suspended in the air, fog usually appears when
449 water vapor becomes saturated as the temperature drops below the dew point. The formation of
450 fog needs abundant water vapor and specific temperature conditions. The Sichuan Basin has a low
451 altitude and high temperature, producing abundant water vapor through intense evaporation (Rong
452 et al., 2012). With a relative flat topography, the southern edge of the basin provides a main
453 pathway for water vapor transport out of the basin. The variation of seasonal prevailing wind
454 direction (supporting information Figure S7) indicates that the study area receives water vapor
455 from both Sichuan Basin and southeastern areas throughout the whole year. The river valley of the
456 downstream Chishui River provides a natural channel for water vapor movement (Figure 7).

457 The outcropped strata are dominated by Jurassic mudstone, shale and limestone in the
458 southern part of the Sichuan Basin, and Triassic limestone and dolomite in the northern part of the
459 Yunnan-Guizhou Plateau. However, the study site is mainly underlain by Cretaceous or Jurassic
460 quartz sandstone, different from surrounding areas (Figure 7). Compared with limestone and other
461 rock types, sandstone has a greater water-holding capacity and weathers more quickly (Goudie et



462 al., 1970; Turkington and Paradise, 2005), which results in soils with better water and nutritional
463 conditions for local plant species to grow and survive (Jiang et al., 2012). As a result, this sandstone
464 area is mostly covered by forest, and has a different landform and microclimate from the
465 surrounding regions. When water vapor from surrounding areas moves towards the Chishui valley,
466 it is uplifted by the topography and cooled, resulting in fog. The forest's regulation on local
467 weather leads to stable air temperature and small wind speed (supporting information Figure S5 &
468 S6), both favoring the formation of forest fog. Usually bigger wind speed results in bigger fog
469 water interception (Prada et al., 2009, 2012), but the small wind speed is also benefit for the
470 occurrence and residence of frequent heavy fog. Moreover, compared with limestone, mudstone,
471 shale and dolomite, the quartz sandstone has a relatively high thermal conductivity and small
472 specific heat capacity (Clauser and Huenges, 1995; Kappelmeyer and Haenel, 1974). This allows
473 a relatively fast drop of near-surface temperature in the Chishui region after sunset, enhancing fog
474 formation.

475 Because of the special geographical location and geological conditions, the Chishui forest
476 region is covered by heavy fog in most days of the year. In arid regions such as northern Kenya,
477 the residents collect fog water for their water supply by installing cooling screens windward
478 (Ingraham and Matthews, 1988). The dense canopy of the Chishui forest, especially in the Datong
479 and Fengxi catchments, functions like a natural screen to capture fog water droplets from the air
480 and produce larger water drops that subsequently fall to the forest ground. Some of the fog water
481 is lost via evapotranspiration while the rest infiltrates into soils together with rainwater and
482 recharges local groundwater. Rainwater can saturate the soils and form near-surface flow and
483 quickly enter surface water in the rainy season with abundant and intense rainfall, but mainly
484 infiltrates and recharges groundwater that leads to baseflow in the dry period. Unlike rainwater,
485 fog water recharge is persistent and despite its relatively low intensity, leads to considerable water
486 input throughout the year.

487 Sedimentary sandstone in the Chishui forest region has obvious layering and is made up of
488 sand particles with different sizes (Figure 2c), causing certain differences in compactness and
489 permeability (Peng, 2001). When the groundwater stored in the sandstone (suspended aquifers)
490 comes across the argillaceous sandstone layers that have relatively smaller permeability, it will
491 move along these structures and finally flow out as spring water (Figure 2g). Such springs exist
492 throughout the valleys, forming large numbers of streams which become waterfalls at geological



493 escarpments. Although the rainfall amount in the study area is similar to the surrounding areas
494 (supporting information Figure S4), fog water provides considerable recharge to groundwater. As
495 a consequence, groundwater can maintain the large discharge of waterfalls during a long dry period.
496 The special geographical location, geological and lithologic characteristics, as well as the
497 vegetation conditions of the Chishui forest region together create this unique waterfall landscape.
498 How the area developed such a landscape under combined influences of various interacting factors
499 over time would be an interesting question for future research to better understand the interactions
500 among hydrological, geological and ecological processes in the evolution of an earth system.

501 **4 Concluding remarks**

502 Isotopic signatures of stream water, fog water and rainfall in the Chishui forest indicate that
503 frequent fog drip is a key water source for sustaining streamflow and plays an important role in
504 the regional ecohydrology. Since the forest is located in the vapor passage in the southern part of
505 the Sichuan Basin, abundant water vapor from the basin and southeastern regions provides an
506 essential condition for the fog formation. The special properties of sandstone strata create a thick
507 forest landscape and a microclimate that also favor the formation of frequent fogs in the study area.
508 Seven-month monitoring of the isotopes in streams fed by water from waterfalls in the catchments
509 indicates that surface water flow is formed by subsurface runoff with different proportions of
510 groundwater and near-surface flow in different time periods. During the dry period starting around
511 October, surface water that forms thousands of waterfalls is mainly sustained by baseflow, 8-31%
512 of which comes from the frequent fog water recharge. Fog is intercepted by the leaves of forest
513 plants and forms large water drops that fall to the ground, infiltrate the soil and recharge
514 groundwater together with rainwater. Groundwater flows out of sandstone layers and forms springs,
515 which then converge into streams and waterfalls. Overall, fog water provides 98-504 mm/a
516 recharge to the hydrologic system, in addition to the rainfall input (1122 mm in 2015).

517 The present study, based on the isotope method, has demonstrated that fog water contributes
518 significantly to the water balance and contributes to baseflow in the waterfall landscape in the
519 Chishui forest region. This unique waterfall landscape is inseparable from the geographical
520 location, geological activities, lithologic characters as well as the vegetation conditions. We
521 suggest that future investigations should be carried out with long-term measurements of isotopes
522 and hydrological parameters, including river flow, local rainfall and fog water dripping rate, to



523 further explore the processes underlying the behavior and evolution of this complex
524 ecohydrological system.

525 **Acknowledgments**

526 Data used in this study are included in the supporting information. This research was funded by
527 the National Natural Science Foundation of China (51578212) and the National Basic Research
528 Program of China (2012CB417005). We gratefully acknowledge the funding from the China
529 Scholarship Council. We thank laboratory technician Zhiguo Su for the isotopic analysis of
530 samples. We also thank Shiyin Zhang, Jin Geng, Wencheng Tao, Hongbo Zhao for their assistance
531 in collecting field samples.

532 **References**

- 533 Aboal, J. R., Jim énez, M. S., Morales, D. and Gil, P.: Effects of thinning on throughfall in Canary
534 Islands pine forest - The role of fog, *J. Hydrol.*, 238(3–4), 218–230, doi:10.1016/S0022-
535 1694(00)00329-2, 2000.
- 536 Bruijnzeel, L. A.: Hydrology of tropical montane cloud forests: a reassessment., Gladwell, J.S.
537 (Ed.), *Proc. Second Int. Colloq. Hydrol. Water Manag. Humid Trop.* UNESCO, Paris
538 CATHALAC, Panama Ci, (January 2001), 2002.
- 539 Bruijnzeel, L. A., Mulligan, M. and Scatena, F. N.: Hydrometeorology of tropical montane cloud
540 forests: Emerging patterns, *Hydrol. Process.*, 25(3), 465–498, doi:10.1002/hyp.7974, 2011.
- 541 Cavelier, J., Solis, D. and Jaramillo, M. A.: Fog interception in montane forests across the Central
542 Cordillera of Panamá *J. Trop. Ecol.*, 12(3), 357–369, doi:10.1017/S026646740000955X, 1996.
- 543 Chang, S. C., Yeh, C. F., Wu, M. J., Hsia, Y. J. and Wu, J. T.: Quantifying fog water deposition
544 by in situ exposure experiments in a mountainous coniferous forest in Taiwan, *For. Ecol. Manage.*,
545 224(1–2), 11–18, doi:10.1016/j.foreco.2005.12.004, 2006.
- 546 Chen, J.: Study on the forming conditions in first class waterfall of Danxia in China-Shizhangdong
547 of Chishui, *Guizhou Sci.*, 21(4), 63–67, 2003.
- 548 Chen, J., Liu, X., Sun, X., Su, Z. and Yong, B.: The origin of groundwater in Zhangye Basin,
549 northwestern China, using isotopic signature, *Hydrogeol. J.*, 22(1), 411–424, doi:10.1007/s10040-
550 013-1051-7, 2014.



- 551 Clauser, C. and Huenges, E.: Thermal Conductivity of Rocks and Minerals, *Rock Phys. Phase*
552 *Relations*, 105–126, doi:10.1029/RF003p0105, 1995.
- 553 Corbin, J. D., Thomsen, M. A., Dawson, T. E. and D’Antonio, C. M.: Summer water use by
554 California coastal prairie grasses: Fog, drought, and community composition, *Oecologia*, 145(4),
555 511–521, doi:10.1007/s00442-005-0152-y, 2005.
- 556 Dawson, T. E.: Fog in the California redwood forest: Ecosystem inputs and use by plants,
557 *Oecologia*, 117(4), 476–485, doi:10.1007/s004420050683, 1998.
- 558 Del-Val, E., Armesto, J. J., Barbosa, O., Christie, D. A., Gutiérrez, A. G., Jones, C. G., Marquet,
559 P. A. and Weathers, K. C.: Rain forest islands in the Chilean semiarid region: Fog-dependency,
560 ecosystem persistence and tree regeneration, *Ecosystems*, 9(4), 598–608, doi:10.1007/s10021-
561 006-0065-6, 2006.
- 562 Eugster, W., Burkard, R., Holwerda, F., Scatena, F. N. and Bruijnzeel, L. A. (Sampurno):
563 Characteristics of fog and fogwater fluxes in a Puerto Rican elfin cloud forest, *Agric. For.*
564 *Meteorol.*, 139(3–4), 288–306, doi:10.1016/j.agrformet.2006.07.008, 2006.
- 565 Figueira, C., Sequeira, M. M., Vasconcelos, R. and Prada, S.: Cloud water interception in the
566 temperate laurel forest of Madeira Island, *Hydrol. Sci. J.*, 58(1), 152–161,
567 doi:10.1080/02626667.2012.742952, 2013.
- 568 Fischer, D. T., Still, C. J., Ebert, C. M., Baguskas, S. A. and Williams, A. P.: Fog drip maintains
569 dry season ecological function in a California coastal pine forest, *Ecosphere*, 7(6), 1–21,
570 doi:10.1002/ecs2.1364, 2016.
- 571 Froehlich, K., Kralik, M., Papesch, W., Rank, D., Scheifinger, H. and Stichler, W.: Deuterium
572 excess in precipitation of Alpine regions - moisture recycling., *Isotopes Environ. Health Stud.*,
573 44(1), 61–70, doi:10.1080/10256010801887208, 2008.
- 574 Garc ía-Santos, G. and Bruijnzeel, L. A.: Rainfall, fog and throughfall dynamics in a subtropical
575 ridge top cloud forest, National Park of Garajonay (La Gomera, Canary Islands, Spain), *Hydrol.*
576 *Process.*, 25(3), 411–417, doi:10.1002/hyp.7760, 2011.
- 577 Goldstein, G., Meinzer, F. C., Bucci, S. J., Scholz, F. G., Franco, A. C. and Hoffmann, W. a: Water
578 economy of Neotropical savanna trees: six paradigms revisited, *Tree Physiol.*, 28(3), 395–404,
579 doi:10.1093/treephys/28.3.395, 2008.



- 580 Gonfiantini, R. and Longinelli, A.: Oxygen isotopic composition of fogs and rains from the North
581 Atlantic, *Experientia*, 18(5), 222–223, doi:10.1007/BF02148311, 1962.
- 582 Goni, I. B.: Tracing stable isotope values from meteoric water to groundwater in the southwestern
583 part of the Chad basin, *Hydrogeol. J.*, 14(5), 742–752, doi:10.1007/s10040-005-0469-y, 2006.
- 584 Goudie, A., Cooke, R. and Evans, I.: Experimental investigation of rock weathering by salts, *Area*,
585 2(4), 42–48 (online) Available from: <http://www.jstor.org/stable/10.2307/20000488>, 1970.
- 586 Holder, C. D.: Rainfall interception and fog precipitation in a tropical montane cloud forest of
587 Guatemala, *For. Ecol. Manage.*, 190(2–3), 373–384, doi:10.1016/j.foreco.2003.11.004, 2004.
- 588 Hutley, L. B., Doley, D., Yates, D. and Boonsaner, A.: Water balance of an Australian subtropical
589 rainforest at altitude: the ecological and physiological significance of intercepted cloud and fog,
590 *Aust. J. Bot.*, 45(2), 311–329, doi:10.1071/BT96014, 1997.
- 591 Imteaz, M. A., Al-Hassan, G., Shanableh, A. and Naser, J.: Development of a mathematical model
592 for the quantification of fog-collection, *Resour. Conserv. Recycl.*, 57, 10–14,
593 doi:10.1016/j.resconrec.2011.09.014, 2011.
- 594 Ingraham, N. L. and Mark, A. F.: Isotopic assessment of the hydrologic importance of fog
595 deposition on tall snow tussock grass on southern New Zealand uplands, *Austral Ecol.*, 25(4), 402–
596 408, doi:10.1046/j.1442-9993.2000.01052.x, 2000.
- 597 Ingraham, N. L. and Matthews, R. A.: Fog drip as a source of groundwater recharge in northern
598 Kenya, *Water Resour. Res.*, 24(8), 1406–1410, doi:10.1029/WR024i008p01406, 1988.
- 599 Ingraham, N. L. and Matthews, R. A.: A stable isotopic study of fog: the Point Reyes Peninsula,
600 California, U.S.A., *Chem. Geol. Isot. Geosci. Sect.*, 80(4), 281–290, doi:10.1016/0168-
601 9622(90)90010-A, 1990.
- 602 Jackson, P. C., Cavelier, J., Goldstein, G., Meinzer, F. C. and Holbrook, N. M.: Partitioning of
603 water resources among plants of a lowland tropical forest, *Oecologia*, 101(2), 197–203,
604 doi:10.1007/BF00317284, 1995.
- 605 Jiang, M., Zhang, S. and Su, L.: A brief talk on relation of vegetation with stratigraphy and its
606 geological significance, *Acta Geol. Sichuan*, 32(2), 2–4, doi:10.3969/j.issn.1006-
607 0995.2012.02.018, 2012.



- 608 Kappelmeyer, O. and Haenel, R.: Geothermics with special reference to applications, in Berlin
609 Gebrueder Borntraeger Geoexploration Monographs Series, vol. 4, p. 238., 1974.
- 610 Klaus, J. and McDonnell, J. J.: Hydrograph separation using stable isotopes: Review and
611 evaluation, *J. Hydrol.*, 505, 47–64, doi:10.1016/j.jhydrol.2013.09.006, 2013.
- 612 Klemm, O., Schemenauer, R. S., Lummerich, A., Cereceda, P., Marzol, V., Corell, D., Van
613 Heerden, J., Reinhard, D., Gherezghiher, T., Olivier, J., Osses, P., Sarsour, J., Frost, E., Estrela,
614 M. J., Valiente, J. A. and Fessehaye, G. M.: Fog as a fresh-water resource: Overview and
615 perspectives, *Ambio*, 41(3), 221–234, doi:10.1007/s13280-012-0247-8, 2012.
- 616 Li, X., He, Q., Dong, Y., Cao, X., Wang, Z. and Duan, X.: An analysis of characteristics and
617 evolution of Danxia landform in the south of Chishui county , Guizhou, *Acta Geosci. Sin.*, 34(4),
618 501–508, doi:10.3975/cagsb.2013.04.14, 2013a.
- 619 Li, X., Dong, Y., Li, C. and Cao, X.: Characteristics and assessment of geological heritages in
620 Chishui Danxia national geopark in Guizhou province, *Chinese J. Geol. Hazard Control*, 24(1),
621 118–125, doi:10.16031/j.cnki.issn.1003-8035.2013.01.007, 2013b.
- 622 Liu, W., Meng, F., Zhang, Y., Liu, Y. and Li, H.: Water input from fog drip in the tropical seasonal
623 rain forest of Xishuangbanna, South-West China, *J. Trop. Ecol.*, 20(5), 517–524,
624 doi:10.1017/S0266467404001890, 2004.
- 625 Liu, W., Li, P., Duan, W. and Liu, W.: Dry-season water utilization by trees growing on thin karst
626 soils in a seasonal tropical rainforest of Xishuangbanna, Southwest China, *Ecohydrology*, 7(3),
627 927–935, doi:10.1002/eco.1419, 2014.
- 628 Liu, W. J., Ping Zhang, Y., Mei Li, H. and Hong Liu, Y.: Fog drip and its relation to groundwater
629 in the tropical seasonal rain forest of Xishuangbanna, Southwest China: A preliminary study,
630 *Water Res.*, 39(5), 787–794, doi:10.1016/j.watres.2004.12.002, 2005.
- 631 Liu, W. J., Liu, W. Y., Li, P. J., Gao, L., Shen, Y. X., Wang, P. Y., Zhang, Y. P. and Li, H. M.:
632 Using stable isotopes to determine sources of fog drip in a tropical seasonal rain forest of
633 Xishuangbanna, SW China, *Agric. For. Meteorol.*, 143(1–2), 80–91,
634 doi:10.1016/j.agrformet.2006.11.009, 2007.



- 635 Liu, Z., Tian, L., Yao, T. and Yu, W.: Seasonal deuterium excess in Nagqu precipitation: Influence
636 of moisture transport and recycling in the middle of Tibetan Plateau, *Environ. Geol.*, 55(7), 1501–
637 1506, doi:10.1007/s00254-007-1100-4, 2008.
- 638 Meyer, S. C.: Analysis of base flow trends in urban streams, Northeastern Illinois, USA,
639 *Hydrogeol. J.*, 13(5–6), 871–885, doi:10.1007/s10040-004-0383-8, 2005.
- 640 Muñoz-Villers, L. E. and McDonnell, J. J.: Runoff generation in a steep, tropical montane cloud
641 forest catchment on permeable volcanic substrate, *Water Resour. Res.*, 48(9), 1–17,
642 doi:10.1029/2011WR011316, 2012.
- 643 Nagel, J. F.: Fog precipitation on table mountain, *Q. J. R. Meteorol. Soc.*, 82(354), 452–460,
644 doi:10.1002/qj.49708235408, 1956.
- 645 Palacio, S., Azorín, J., Montserrat-Martí G. and Ferrio, J. P.: The crystallization water of gypsum
646 rocks is a relevant water source for plants, *Nat. Commun.*, 5, 4660, doi:10.1038/ncomms5660,
647 2014.
- 648 Peng, H.: Danxia geomorphology of China: A review, *Chinese Sci. Bull.*, 46(S1), 38–44,
649 doi:10.1007/BF03187234, 2001.
- 650 Phillips, D. L. and Gregg, J. W.: Uncertainty in source partitioning using stable isotopes, *Oecologia*,
651 127(2), 171–179, doi:10.1007/s004420000578, 2001.
- 652 Poage, M. A. and Chamberlain, C. P.: Empirical relationships between elevation and the stable
653 isotope composition of precipitation and surface waters: Considerations for studies of
654 paleoelevation change, *Am. J. Sci.*, 301(1), 1–15, doi:10.2475/ajs.301.1.1, 2001.
- 655 Prada, S., Menezes de Sequeira, M., Figueira, C. and da Silva, M. O.: Fog precipitation and rainfall
656 interception in the natural forests of Madeira Island (Portugal), *Agric. For. Meteorol.*, 149(6),
657 1179–1187, doi:10.1016/j.agrformet.2009.02.010, 2009.
- 658 Prada, S., De Sequeira, M. M., Figueira, C. and Vasconcelos, R.: Cloud water interception in the
659 high altitude tree heath forest (*Erica arborea* L.) of Paul da Serra Massif (Madeira, Portugal),
660 *Hydrol. Process.*, 26(2), 202–212, doi:10.1002/hyp.8126, 2012.



- 661 Prada, S., Figueira, C., Aguiar, N. and Cruz, J. V.: Stable isotopes in rain and cloud water in
662 Madeira: contribution for the hydrogeologic framework of a volcanic island, *Environ. Earth Sci.*,
663 73(6), 2733–2747, doi:10.1007/s12665-014-3270-1, 2015.
- 664 Prada, S., Cruz, J. V. and Figueira, C.: Using stable isotopes to characterize groundwater recharge
665 sources in the volcanic island of Madeira, Portugal, *J. Hydrol.*, 536, 409–425,
666 doi:10.1016/j.jhydrol.2016.03.009, 2016.
- 667 Qi, D., Yu, R., Zhang, R., Ge, Y. and Li, J.: Comparative studies of Danxia landforms in China, *J.*
668 *Geogr. Sci.*, 15(3), 337–345, doi:10.1007/BF02837521, 2005.
- 669 Querejeta, J. I., Estrada-Medina, H., Allen, M. F. and Jiménez-Osornio, J. J.: Water source
670 partitioning among trees growing on shallow karst soils in a seasonally dry tropical climate,
671 *Oecologia*, 152(1), 26–36, doi:10.1007/s00442-006-0629-3, 2007.
- 672 Ritter, A., Regalado, C. M. and Aschan, G.: Fog water collection in a subtropical elfin laurel forest
673 of the Garajonay National Park (Canary Islands): a combined approach using artificial fog catchers
674 and a physically based impaction model, *J. Hydrometeorol.*, 9(5), 920–935,
675 doi:10.1175/2008JHM992.1, 2008.
- 676 Rong, Y., Zhang, X., Jiang, H. and Bai, L.: Pan evaporation change and its impact on water cycle
677 over the upper reach of Yangtze River, *Chinese J. Geophys.*, 55(5), 488–497,
678 doi:10.1002/cjg2.1744, 2012.
- 679 Schmid, S., Burkard, R., Frumau, K. F. A., Tobón, C., Bruijnzeel, L. A., Siegwolf, R. and Eugster,
680 W.: Using eddy covariance and stable isotope mass balance techniques to estimate fog water
681 contributions to a Costa Rican cloud forest during the dry season, *Hydrol. Process.*, 25(3), 429–
682 437, doi:10.1002/hyp.7739, 2011.
- 683 Scholl, M., Eugster, W. and Burkard, R.: Understanding the role of fog in forest hydrology: Stable
684 isotopes as tools for determining input and partitioning of cloud water in montane forests, *Hydrol.*
685 *Process.*, 25(3), 353–366, doi:10.1002/hyp.7762, 2011.
- 686 Turkington, A. V. and Paradise, T. R.: Sandstone weathering: A century of research and innovation,
687 *Geomorphology*, 67(1), 229–253, doi:10.1016/j.geomorph.2004.09.028, 2005.



688 Uehara, Y. and Kume, A.: Canopy rainfall interception and fog capture by *Pinus pumila* regal at
689 Mt. Tateyama in the northern Japan alps, Japan, Arctic, Antarct. Alp. Res., 44(1), 143–150,
690 doi:10.1657/1938-4246-44.1.143, 2012.

691 Vogelmann, H. W., Siccama, T., Leedy, D. and Ovitt, D. C.: Precipitation from fog moisture in
692 the Green Mountains of Vermont, Ecology, 49(6), 1205–1207, doi:10.2307/1934518, 1968.

693 Xu, X., Mu, B., He, P. and Xiong, Z.: Analysis and evaluation on climate resource for tourism of
694 Chishui landscape spot, J. Guizhou Univ., 21(5), 320–326, 2002.

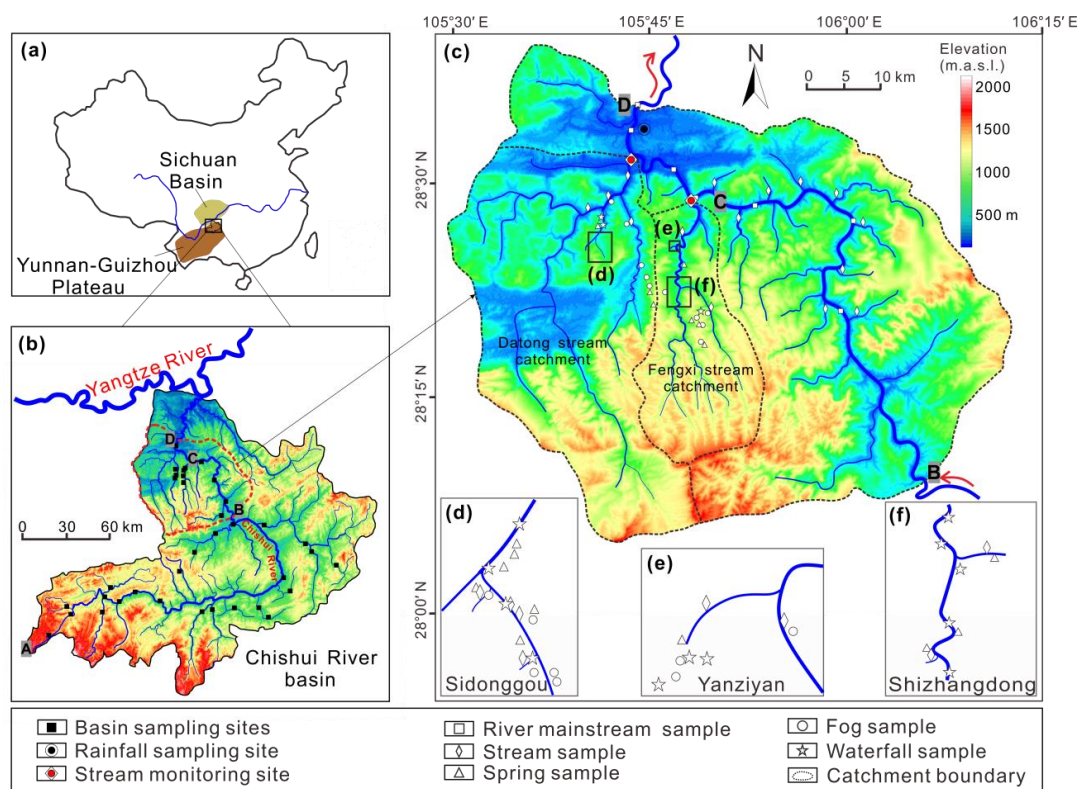
695 Yang, G., An, Y. and Tu, Y.: Investigation of eco-environment in Chishui Alsophila Natural
696 Reserve based on GIS & RS, J. Cent. South Univ. For. Technol., 31(11), 125–130,
697 doi:10.14067/j.cnki.1673-923x.2011.11.035, 2011.

698 Zhan, L., Chen, J., Zhang, S., Li, L., Huang, D. and Wang, T.: Isotopic signatures of precipitation,
699 surface water, and groundwater interactions, Poyang Lake Basin, China, Environ. Earth Sci.,
700 75(19), 1–14, doi:10.1007/s12665-016-6081-8, 2016.

701 Zhan, L., Chen, J. and Li, L.: Isotopic assessment of fog drip water contribution to vegetation
702 during dry season in Junshan wetland, northern Dongting Lake, Wetl. Ecol. Manag., 25(3), 345–
703 357, doi:10.1007/s11273-016-9521-z, 2017.

704

705



706

707

708

709

710

711

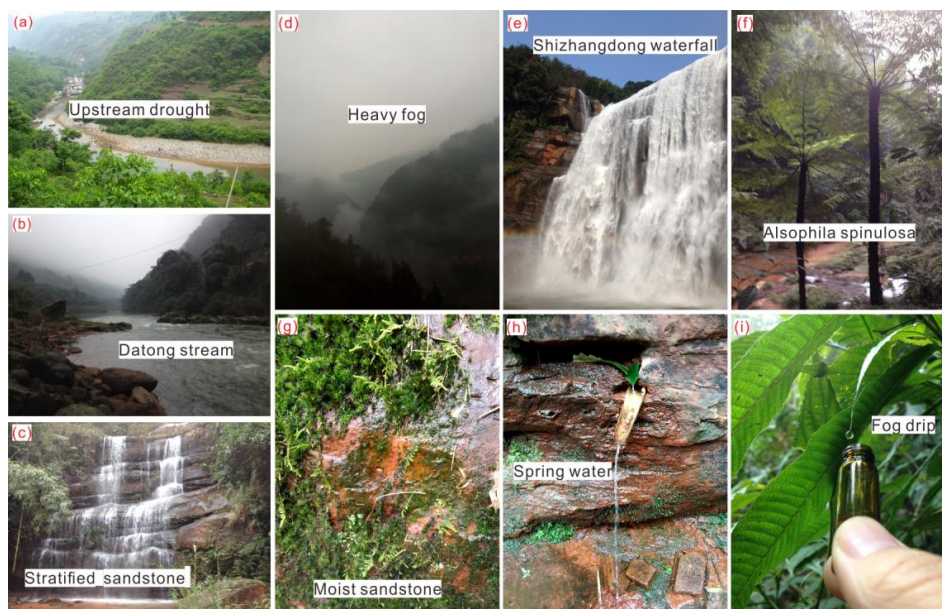
712

713

714

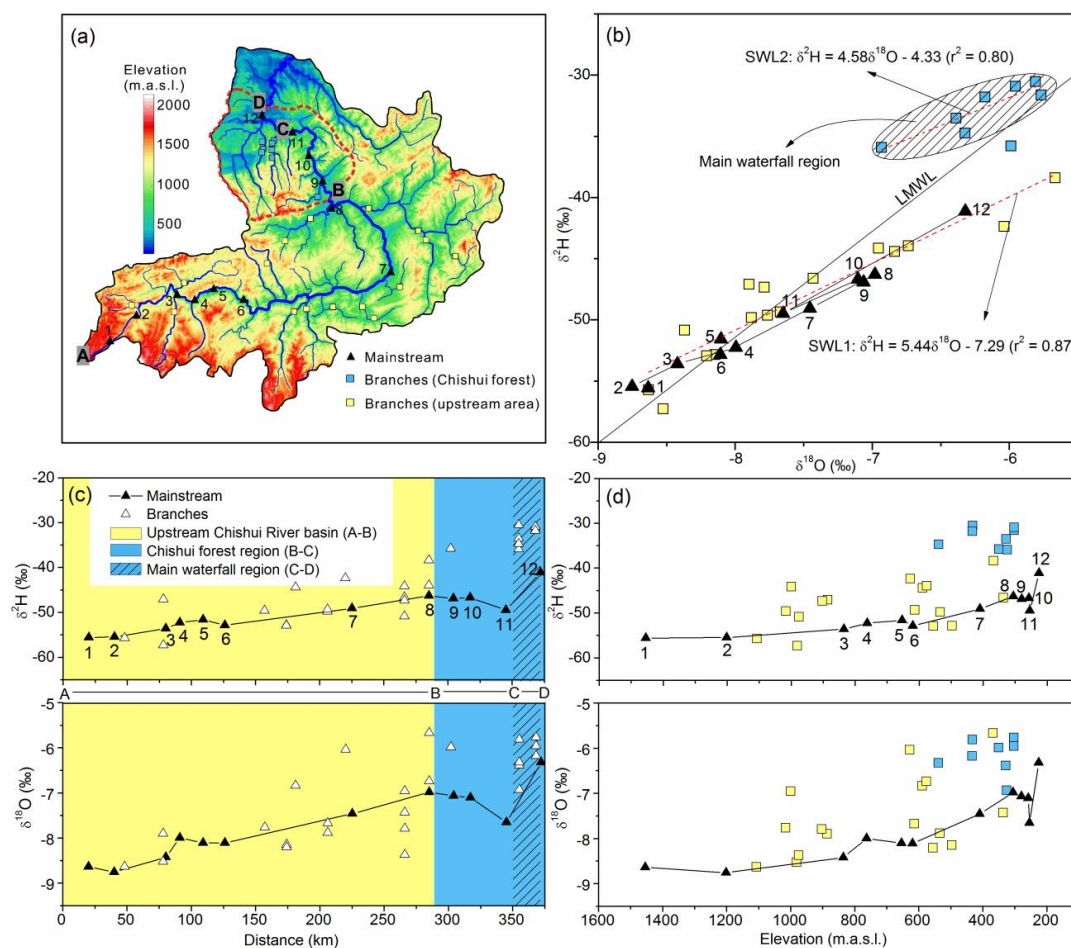
715

Figure 1. Location of the study area and sites for water sampling in the Chishui River basin and Chishui forest catchment. (a) Study area located in the transition zone between the Yunnan-Guizhou Plateau and the Sichuan Basin in the southwest of China. (b) Sampling sites (June 2011) in the Chishui River basin and the location of the Chishui forest catchment. (c) Sampling sites (December 2014) in the Chishui forest catchment, including the Datong and Fengxi stream catchments (main waterfall area). (d) Sampling sites in Sidonggou waterfall landscape area. (e) Sampling sites in Yanziyan waterfall landscape area. (f) Sampling sites in Shizhangdong waterfall landscape area. The digital elevation data are sourced from China Geospatial Data Cloud (<http://www.gscloud.cn/>).



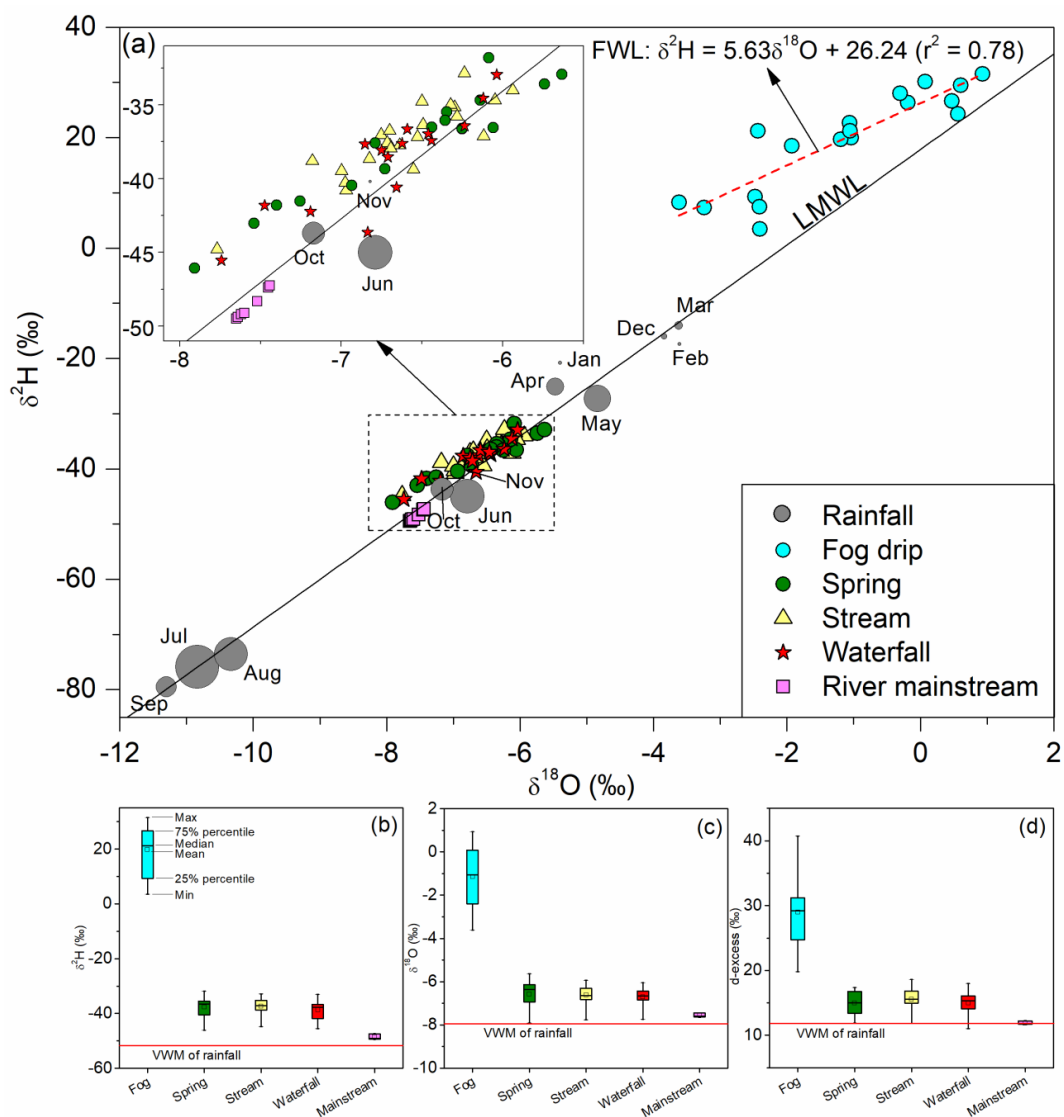
716

717 **Figure 2.** Pictures taken during the field investigation and sampling. (a) Small stream discharge
718 in the upstream catchments of the Chishui River due to the drought in the spring of 2011. (b) A
719 photo taken in June 2011, showing the fog occurrence and the large discharge in the Datong stream
720 in contrast with the upstream situation shown in (a). (c) Photo of a small waterfall on the stratified
721 sandstone taken during the first field investigation. (d) Heavy fog during the second field
722 investigation in December 2014. (e) The biggest waterfall (105°44'27.52" E, 28°21'35.14" N) in
723 the study area photographed in December 2014. (f) *Alsophila spinulosa*, an ancient species
724 surviving since the dinosaur age, grows in the study area. (g) Red sandstone under the forest
725 canopy wetted by fog water drops. (h) Spring water flowing out from the fissures of sandstone. (i)
726 Sampling fog water by collecting water drops on the tips of plant leaves under the forest canopy.



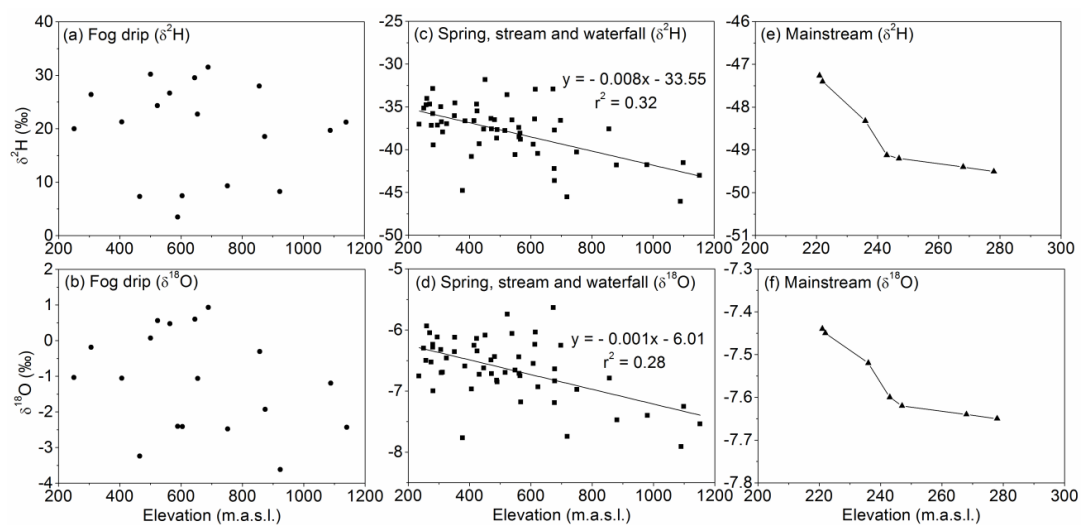
727

728 **Figure 3.** Isotopic characteristics of surface water in the Chishui River basin based on water
 729 samples collected in June 2011. (a) Sampling sites of the Chishui River mainstream (No.1 to 12)
 730 and its tributaries/branches. (b) The relationship between $\delta^{18}\text{O}$ and $\delta^2\text{H}$ values. (c) Isotopic
 731 variations of surface water along the Chishui River basin. (d) The relationship between isotopic
 732 values and sampling elevations. The local meteoric water line (LMWL) was fitted for monthly
 733 rainfall samples collected in 2015 (supporting information Figure S2). The x axis of (c) stands for
 734 the distance from the river headstream (A) to each sampling location along the mainstream or each
 735 junction of the mainstream and branch. SWL stands for surface water line.



736

737 **Figure 4.** Relationship between $\delta^{18}\text{O}$ and $\delta^2\text{H}$ (a) of all water samples collected in the Chishui
 738 forest catchment during the sampling campaign conducted in December 2014, and box plots of
 739 $\delta^2\text{H}$ (b), $\delta^{18}\text{O}$ (c) and d-excess (d) values for different water types. The sizes of dark grey circles
 740 in (a) represent the relative amount of rainfall in different months. FWL stands for the fog water
 741 line and VWM for the volume weighted mean.

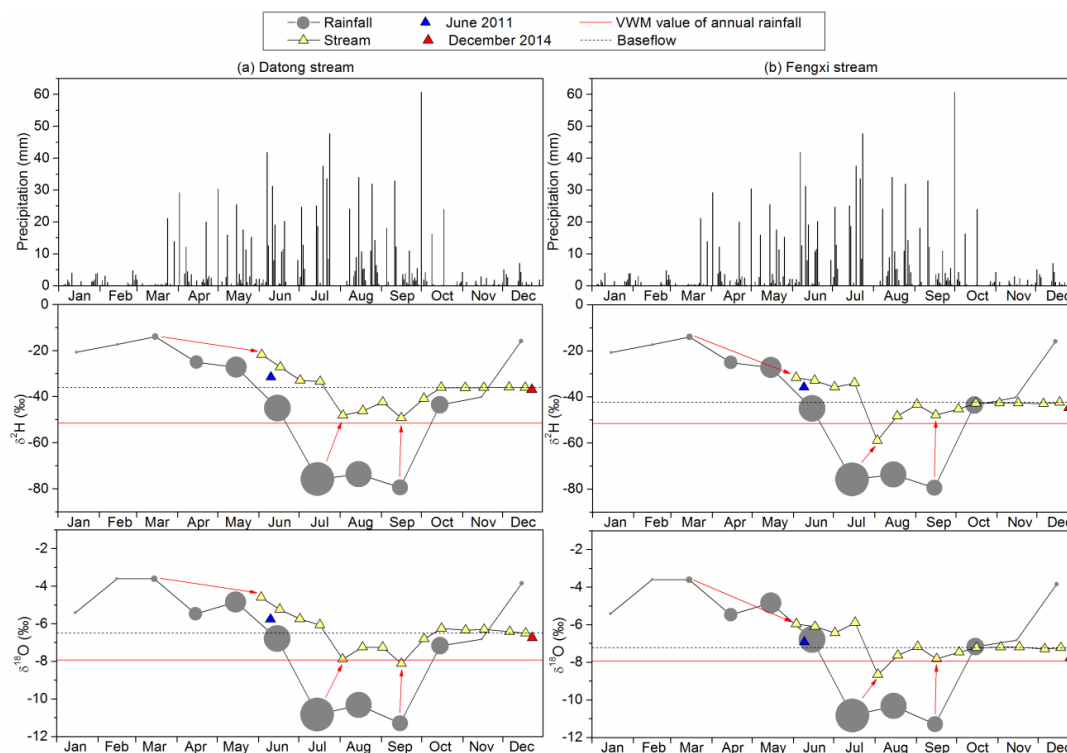


742

743

744

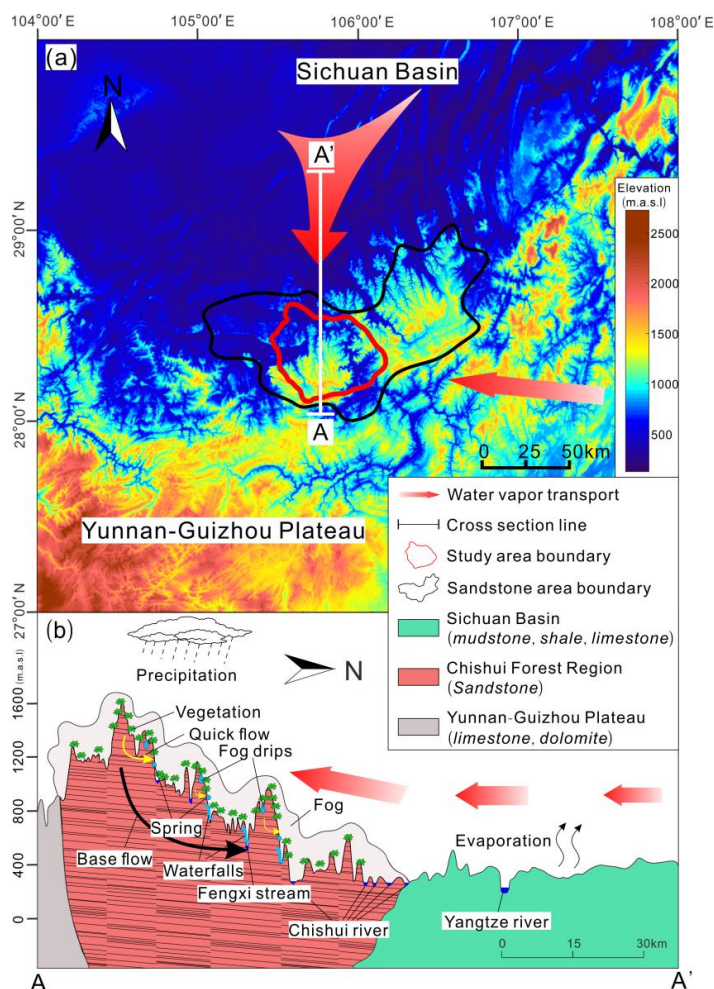
Figure 5. Relationships between isotopic values and corresponding elevations for fog drip, spring, stream, waterfall, and the Chishui River mainstream water samples collected in December 2014.



745

746 **Figure 6.** Comparison of monthly variations of isotopic compositions between precipitation and
 747 water from Datong and Fengxi streams in 2015. Daily rainfall data at a nearby meteorological
 748 station in the study area (Figure S3, about 35 km away from the Fengxi catchment) were obtained
 749 from China Meteorological Database (<http://data.cma.cn/>). The sizes of dark grey circles represent
 750 the relative amount of rainfall. The volume-weighted mean (VWM) isotopic values of monthly
 751 rainfall were calculated using monthly rainfall isotopes and monthly rainfall amount in 2015. The
 752 isotopic compositions of baseflow in the two catchments were correspondingly represented by the
 753 isotopic values of stream samples collected in mid-December 2015.

754



755
 756 **Figure 7.** Map of the site and surrounding areas, and diagram of fog formation and hydrologic
 757 process in the study site. (a) Digital elevation map of the transition zone between the Yunnan-
 758 Guizhou Plateau and the Sichuan Basin, as well as the boundaries of Danxia (red sandstone)
 759 landscape and study area. (b) A simplified geological cross-section (A-A') shown in (a) describing
 760 the water vapor source for fogs and the concept model of fog recharge process in the study
 761 catchment. The geological information is obtained from China Geological Information Data
 762 Centre (<http://geodata.ngac.cn/>). The digital elevation data is from China Geospatial Data Cloud
 763 (<http://www.gscloud.cn/>).



764 **Table 1 Isotopic compositions of the end members for the mixing model of baseflow and calculated**
 765 **proportions of fog water input in Datong and Fengxi catchments.**

Catchment	δ_{baseflow} (‰)		$\delta_{\text{rain_VWM}}$ (‰)		δ_{fog} (‰)		X (%)	
	$\delta^2\text{H}$	$\delta^{18}\text{O}$	$\delta^2\text{H}$	$\delta^{18}\text{O}$	$\delta^2\text{H}$	$\delta^{18}\text{O}$	Calculated by $\delta^2\text{H}$	Calculated by $\delta^{18}\text{O}$
Datong	-36.2	-6.50	-51.6	-7.94	22.3±3.0 (3.5-31.5, N=10)	-0.61±0.43 (-3.24-0.93, N=10)	21±1.0 (19-28)	20±1.5 (16-31)
Fengxi	-42.4	-7.23	-51.6	-7.94	16.6±2.5 (7.5-26.6, N=8)	-1.83±0.44 (-3.62-0.47, N=8)	14±0.5 (12-16)	12±0.8 (8-16)

766 Note: The rainwater input was represented by the volume weighted mean (VWM) isotopic values of 12 monthly
 767 rainfall collected in 2015. Mean values with standard errors for fog water isotopic composition and its proportions (X)
 768 in the baseflow were shown, as well as the minimum and maximum (in parentheses). Detailed results for every fog
 769 water sample can be found in the supporting information Database.



770

Table 2 Estimation of fog deposition rate in foggy forests around the world.

Study	Location	Latitude	Longitude	Forest type	Annual rainfall (mm)	Annual fog water input (mm)	Fog proportion, X (%)
Cavelier et al., 1996	Central Cordillera of Panama	8 °41'23"N	82 °11'28"W	Tropical montane forest	3355-5759	142–2295	2.4-60.6
Hutley et al., 1997	Queensland, Australia	28 °13'55"S	152 °25'23"E	Subtropical rainforest	1125	450	40
Dawson, 1998	Northern California	41 °33'N	124 °4'W	Costal redwood forest	1315	224–447	17–34
Holder, 2004	Guatemala	15 °5'57"N	90 °3'59"W	Tropical montane cloud forest	—	270	—
Liu et al., 2004	Xishuangbanna, China	21 °55'39"N	101 °15'55"E	Tropical rainforest	1718	89.4	5
Chang et al., 2006	Taiwan	24 °35'N	121 °25'E	Mountainous coniferous forest	2940	328	10
Eugster et al., 2006*	Puerto Rico	18 °16'17"N	65 °45'39"E	Tropical montane cloud forest	—	1591	13
Del-Val et al., 2006	Chile semiarid region	30 °40'S	71 °30'W	Costal rainforest	147	200	58
Ritter et al., 2008	Canary Islands	28 °8'20"N	17 °15'25"W	Subtropical elfin laurel forest	635–1088	251–281	21-28
Prada et al., 2009	Madeira Island	32 °45'37"N	17 °2'50"W	Costal forest	1660	153.4	13
Schmid et al., 2011*	Costa Rican	10 °21'33"N	84 °48'5"W	Montane cloud forest	—	438	5–9
Uehara and Kume, 2012*	Northern Japan	36 °33'58"N	137 °36'22"E	Alpine forest	—	1226	35
This study	Southeaster n China	28 °21'35" N	105 °44'28" E	Montane cloud forest	1122	98–504	8–31

771 — no result shown in the corresponding paper. Results of rainfall and fog water input in the studies are all converted to mm/year
 772 for comparison, although the results of some studies (*) were only given for several months.